Tailoring a 67 attosecond pulse through advantageous phase-mismatch

Kun Zhao,[1] Qi Zhang,[1] Michael Chini,[1] Yi Wu,[1] Xiaowei Wang,[1,2] and Zenghu Chang[1,*]

[1]*Department of Physics and CREOL, University of Central Florida, Orlando, Florida 32816, USA*

[2]*Department of Physics, National University of Defense Technology, Changsha, Hunan, China*

**Corresponding author: Zenghu.Chang@ucf.edu*

Received May 24, 2012; revised July 25, 2012; accepted August 13, 2012;
posted August 13, 2012 (Doc. ID 169268); published September 14, 2012

A single isolated attosecond pulse of 67 as was composed from an extreme UV supercontinuum covering 55–130 eV generated by the double optical gating technique. Phase mismatch was used to exclude the single-atom cutoff of the spectrum that possesses unfavorable attochirp, allowing the positive attochirp of the remaining spectrum to be compensated by the negative dispersion of a zirconium foil. Two algorithms, PROOF and FROG-CRAB, were employed to retrieve the pulse from the experimental spectrogram, yielding nearly identical results.

OCIS codes: 020.2649, 320.6629, 320.7100.

Single isolated attosecond pulses with a record duration of 80 as were previously generated from the cutoff region of the high harmonic spectrum using the amplitude gating [1]. The extreme UV (XUV) continuum produced by double optical gating (DOG) [2] covers both the plateau and cutoff. If the attochirp, which is positive for photon emissions from the short trajectory, is compensated, much shorter attosecond pulses can be obtained [3]. The attochirp is roughly constant over the plateau but increases rapidly at the low ($\omega_X < I_p$) and high energy (approaching $I_p + 3.2U_p$) spectral regions [3]. Here I_p is the ionization potential of the generation atom, U_p is the ponderomotive energy of the driving laser, and ω_X is the XUV photon angular frequency. Atomic units are used unless otherwise specified.

Many metal filters have a broad transmission window in the XUV region. Within the window, the group delay dispersion (GDD) is typically negative at low photon energies and approaches zero or even changes sign at higher energies. A proper filter can be chosen to block the XUV light with $\omega_X < I_p$ but can only provide attochirp compensation in the low-energy part of its transmission window [4–6]. Additional control over the spectrum and phase of the XUV continuum in the high-energy region of the filter window is needed. This can be realized by manipulating the phase-matching conditions. In attosecond pulse generation, the observed spectrum is determined not only by the response of individual atoms, but also by the coherent build-up of XUV photons, which leads to a reduction of the high-harmonic cutoff to $I_p + \alpha U_p$, referred to as the macroscopic cutoff. Here $\alpha < 3.2$ varies with experimental conditions [7–9]. In this letter, we demonstrated that by tuning the generation gas pressure, the spectrum near the high energy end of the filter window, where the attochirp cannot be compensated, can be removed.

The attosecond XUV pulses were generated with DOG and measured with an attosecond streak camera shown in Fig. 1. A magnetic-bottle electron time-of-flight spectrometer (MBES) with a 3-meter-long flight tube was used to achieve high energy resolution, 0.5 eV, over the 0 to 200 eV photoelectron energy range [10]. The strong magnetic field (8000 Gauss) for collimating the electrons was produced by a permanent magnet. The magnetic field in the μ-metal-shielded flight tube was 10 Gauss. Electrons emitted in a 2π sr solid angle toward the flight tube were detected by a microchannel plate (MCP) detector (Jordan TOF Products) with high time resolution (200 ps) [11]. The signal from the MCP was digitized with a high resolution (25 ps) time-to-digital converter (CAEN Technologies).

The near-infrared (NIR) laser pulses of 7 fs and 1.4 mJ centered at 750 nm were produced at 1 kHz repetition rate by a Ti:Sapphire amplifier followed by a Ne-filled hollow fiber and a chirp-mirror compressor. The NIR beam was split into two arms. The major part (90% of the energy) was sent through the DOG optics and focused to a Ne-filled gas cell to produce the isolated attosecond pulses. The focal spot radius was 20 μm, corresponding to a confocal length of 3.5 mm. The 1 mm-long cell was placed 3 mm after the focus to select the short trajectories. The beam waist at the gas cell was about 40 μm. With 0.4 mJ on the target, the peak intensity at the center of the polarization gate in DOG was estimated to be 1×10^{15} W/cm^2. The XUV beam was filtered by a 300 nm Zr foil and focused by a gold-coated toroidal mirror with a 5 deg. glancing incidence angle to a Ne gas jet for pulse duration measurement. The diameter of the jet opening was 50 μm. The streaking NIR beam was recombined with the XUV beam by a hole-drilled mirror, and focused

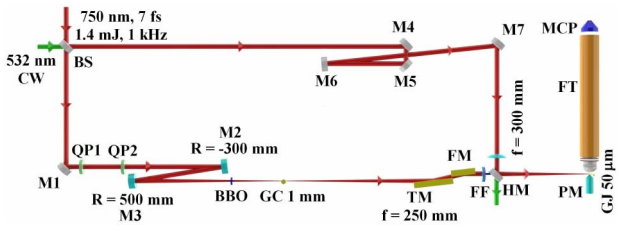

Fig. 1. (Color online) Attosecond streak camera with MBES [10]. BS, beam splitter; QP1 and 2, quartz plates. The thickness of QP1 is 270 μm, giving a polarization gate width of 1.75 fs. M1–M7, silver mirrors; M6, PZT; BBO, second harmonic crystal; GC, gas cell; FF, Zr foil; TM, toroidal mirror; FM, flat mirror; HM, hole-drilled mirror; GJ, gas jet; PM, permanent magnet; FT, flight tube; MCP, electron detector.

by a 300 mm focal length lens. The diameter of the center spot of the focused Bessel streaking beam was 55 μm. The delay between the XUV and NIR pulses was controlled by a piezo-electric transducer (PZT). A 532 nm laser beam co-propagating through both arms was used to stabilize the Mach-Zehnder interferometer [12].

The continuous XUV spectra generated with DOG measured by the MBES without streaking are shown in Fig. 2. By tuning the Ne pressure in the gas cell from 0.03 to 0.33 bar, the cutoff photon energy was reduced from 160 to 120 eV, which corresponds to $I_p + 2.6U_p$ to $I_p + 1.8U_p$. The calculated single-atom cutoff is 190 eV. The spectrum with pressure below 0.03 bar was not measured due to the low count rate. The observed cutoff reduction with increasing generation gas pressure is qualitatively consistent with previous experiments with XUV pulse trains [8,9]. Finally, the pressure of 0.2 bar in the generation cell was chosen for the streaking experiment, where the entire spectrum, from 55 to 130 eV, was confined within the low-energy part of the Zr transmission window where the filter GDD is negative.

The attosecond pulses were retrieved from the streaking trace shown in Fig. 3(a) using both the PROOF (phase retrieval by omega oscillation filtering) [13] and FROG-CRAB (frequency-resolved optical gating for complete reconstruction of attosecond bursts) [14,15] techniques. Whereas the FROG-CRAB technique requires the bandwidth of the photoelectron spectrum to be small compared to its central energy, PROOF is applicable to much broader spectra [13]. Here, we apply the principal component generalized projections algorithm to PROOF [16], which is more robust than the method developed in [13]. In the limit of low streaking intensities, $U_p < \omega_L$, the streaking spectrogram is given by $S(v,\tau) \approx I_0(v) + I_{\omega_L}(v,\tau) + I_{2\omega_L}(v,\tau)$, where I_{ω_L} and $I_{2\omega_L}$ oscillate with the streaking laser frequency, ω_L, and twice the frequency, respectively [13], τ is the delay between the XUV and laser pulses, and v is the photoelectron speed. Since the spectrum and phase information of the attosecond pulses are completely encoded in I_{ω_L}, the amplitude and phase of the XUV pulse are guessed in PROOF to match the modulation depth and phase angle of I_{ω_L}.

The streaking trace was obtained at a low streaking intensity, 2.5×10^{11} W/cm^2, to satisfy the requirements of PROOF. Two methods are used to confirm the correctness of the phase retrieval. The first is to compare the photoelectron spectrum obtained experimentally to the retrieved ones. This criterion was used in the past [17], and is a necessary condition of an accurate retrieval. Another criterion is the agreement between the filtered I_{ω_L} trace from the measured spectrogram and the retrieved one. It is a much stricter requirement than the first one, because the modulation depth and phase angle of I_{ω_L} are determined by both the spectrum and phase, whereas the first method compares a quantity that is dominated by $I_0(v)$, the unstreaked component of the spectrogram. Our retrieval meets both criteria very well, as shown in Figs. 3(c) and 3(b), respectively. Both the FROG-CRAB and PROOF retrievals yield nearly identical temporal profiles with a pulse duration of 67 ± 2 as, as shown in Fig. 3(d), close to the transform-limited value of 62 as. The error bar was obtained following the treatment in [1], by taking each delay slice in the final guessed spectrogram as a separate measurement of the pulse duration. The experiment was repeated at a higher streaking intensity (5×10^{11} W/cm^2) and yielded the same result. With the intrinsic and Zr phase, we calculated a pulse duration of 68 as with the experimental spectrum, in agreement with our retrieved result. At generation gas pressures significantly lower than 0.2 bar, the count rate was not sufficient for obtaining streaking traces with satisfactory signal to noise ratio. Streaking was also performed at higher pressures, which yielded longer pulses due to the reduced spectral bandwidth. For instance, at 0.36 bar, the retrieved pulse duration was 88 as.

Both PROOF and FROG-CRAB assume that only photoelectrons emitted in a small angle in the streaking

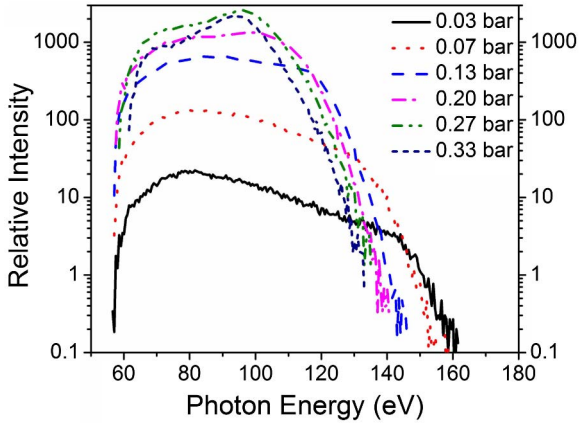

Fig. 2. (Color online) XUV continuum generated by DOG in Ne gas at six pressures. The length of the gas cell is 1 mm. The peak intensity at the center of the polarization gate is 1×10^{15} W/cm^2.

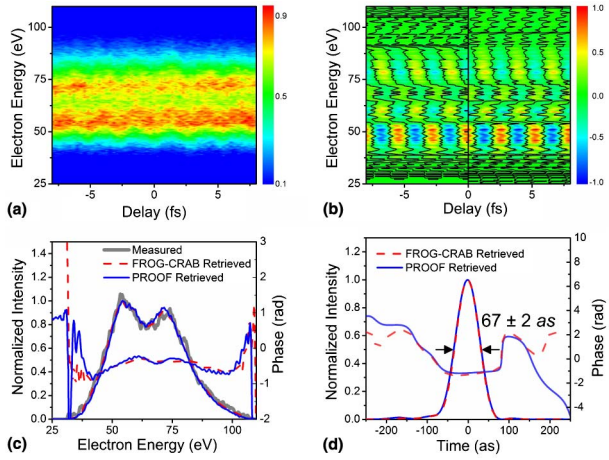

Fig. 3. (Color online) Characterization of a 67 as XUV pulse. (a) Streaked photoelectron spectrogram obtained experimentally. (b) Filtered I_{ω_L} trace (left) from the spectrogram in (a) and the retrieved I_{ω_L} trace (right). (c) Photoelectron spectrum obtained experimentally (thick solid) and retrieved spectra and spectral phases from PROOF (solid) and FROG-CRAB (dashed). (d) Retrieved temporal profiles and phases from PROOF (solid) and FROG-CRAB (dashed).

field direction are collected. However, our MBES collected electrons in 2π sr. When the streaking intensity is low, the dominating Fourier term of the streaking trace that contains the attosecond spectral information is $I_{\omega_L}(v,\tau)$ [13]. It can be shown that $I_{\omega_L}(v,\tau,\theta) = I_{\omega_L}(v,\tau,0)\cos\theta$ for electrons emitted at an angle θ with respect to the flight-tube axis, taking into account the axial symmetry of the photoelectron along the polarization of the streaking field, which is parallel to the flight-tube axis. For a finite collection angle θ_c, $I_{\omega_L}^{(\theta_c)}(v,\tau) \propto \int_0^{\theta_c} I_{\omega_L}(v,\tau,\theta)\rho(\theta)\sin\theta \mathrm{d}\theta \propto I_{\omega_L}(v,\tau,0)$, where $\rho(\theta) = 1+\beta/2(3\cos\theta - 1)$ is the angular distribution of photoelectrons and β is the energy-dependent asymmetric parameter, ranging from 1.33–1.47 between 55 to 130 eV for Ne [18]. This means that $I_{\omega_L}^{(\theta_c)}(v,\tau)$ for an arbitrary θ_c differs from that for $\theta_c = 0$ by only a constant scale factor. This finding is confirmed by simulations. Starting with a 67 as pulse that has the same spectrum and phase as shown in Fig. 3, we numerically created streaking traces with different collection angles from 0 to 90 degrees at the same streaking intensity as in the experiments, using the method described in [15]. The retrieved pulse length from both PROOF and FROG-CRAB algorithms varied less than ± 2 as for all the collection angles, which is within the specified error.

In conclusion, a 67 as XUV pulse, the shortest isolated attosecond pulse to the best of our knowledge, was generated with DOG and fully characterized by PROOF and FROG-CRAB. The retrieved result is consistent with calculated pulse duration based on the experimental spectrum, driving laser intensity, and Zr foil thickness. This plateau spectrum was tailored by utilizing the phase-mismatch to remove the high-energy part of the spectrum with unfavorable chirp and to confine the spectrum to the negative GDD region of the filter. Adjusting the generation gas pressure to utilize advantageous phase-mismatch is an easy-to-implement yet powerful tool for tailoring an XUV spectrum to produce extremely short pulses. This method can be applied to DOG driving by longer wavelength lasers to generate even shorter isolated attosecond pulses.

This material is supported by the U.S. Army Research Office and by the National Science Foundation.

References

1. E. Goulielmakis, M. Schultze, M. Hofstetter, V. S. Yakovlev, J. Gagnon, M. Uiberacker, A. L. Aquila, E. M. Gullikson, D. T. Attwood, R. Kienberger, F. Krausz, and U. Kleineberg, Science **320**, 1614 (2008).
2. H. Mashiko, S. Gilbertson, M. Chini, X. Feng, C. Yun, H. Wang, S. D. Khan, S. Chen, and Z. Chang, Opt. Lett. **34**, 3337 (2009).
3. Z. Chang, Phys. Rev. A **71**, 023813 (2005).
4. B. Henke, E. Gullikson, and J. Davis, Atomic Data and Nuclear Data Tables **54**, 181 (1993).
5. D. H. Ko, K. T. Kim, and C. H. Nam, J. Phys. B **45**, 074015 (2012).
6. R. López-Martens, K. Varjú, P. Johnsson, J. Mauritsson, Y. Mairesse, P. Salières, M. B. Gaarde, K. J. Schafer, A. Persson, S. Svanberg, C.-G. Wahlström, and A. L'Huillier, Phys. Rev. Lett. **94**, 033001 (2005).
7. A. L'Huillier, M. Lewenstein, P. Salières, P. Balcou, M. Y. Ivanov, J. Larsson, and C. G. Wahlström, Phys. Rev. A **48**, R3433 (1993).
8. C. Altucci, T. Starczewski, E. Mevel, C.-G. Wahlström, B. Carré, and A. L'Huillier, J. Opt. Soc. Am. B **13**, 148 (1996).
9. H. Dachraoui, T. Auguste, A. Helmstedt, P. Bartz, M. Michelswirth, N. Mueller, W. Pfeiffer, P. Salieres, and U. Heinzmann, J. Phys. B **42**, 175402 (2009).
10. K. Zhao, Q. Zhang, M. Chini, and Z. Chang, in *Multiphoton Processes and Attosecond Physics*, K. Yamanouchi and K. Midorikawa, eds. (Springer-Verlag, in press).
11. Q. Zhang, K. Zhao, and Z. Chang, Rev. Sci. Instrum. **81**, 073112 (2010).
12. M. Chini, H. Mashiko, H. Wang, S. Chen, C. Yun, S. Scott, S. Gilbertson, and Z. Chang, Opt. Express **17**, 21459 (2009).
13. M. Chini, S. Gilbertson, S. D. Khan, and Z. Chang, Opt. Express **18**, 13006 (2010).
14. Y. Mairesse and F. Quéré, Phys. Rev. A **71**, 011401(R) (2005).
15. H. Wang, M. Chini, S. D. Khan, S. Chen, S. Gilbertson, X. Feng, H. Mashiko, and Z. Chang, J. Phys. B **42**, 134007 (2009).
16. D. J. Kane J. Opt. Soc. Am. B **25**, A120 (2008).
17. G. Sansone, E. Benedetti, F. Calegari, C. Vozzi, L. Avaldi, R. Flammini, L. Poletto, P. Villoresi, C. Altucci, R. Velotta, S. Stagira, S. D. Silvestri, and M. Nisoli, Science **314**, 443 (2006).
18. D. J. Kennedy and S. T. Manson, Phys. Rev. A **5**, 227 (1972).